Journal of Magnetic Resonance **152,** 203–213 (2001)
doi:10.1006/jmre.2001.2420, available online at http://www.idealibrary.com on IDEAL®

Quantitative Evaluation of the Lactate Signal Loss and Its Spatial Dependence in PRESS Localized ^{1}H NMR Spectroscopy

Wulf-Ingo Jung,*,† Michael Bunse,*,† and Otto Lutz†

*Hypertension and Diabetes Research Unit, Max Grundig Clinic, D-77815 Bühl, Germany; and †Physikalisches Institut, University of Tübingen, D-72076 Tübingen, Germany

Received December 12, 2000; revised March 26, 2001; published online September 4, 2001

Localized ^{1}H NMR spectroscopy using the $90^\circ - t_1 - 180^\circ - t_1 + t_2 - 180^\circ - t_2 -$Acq. PRESS sequence can lead to a signal loss for the lactate doublet compared with signals from uncoupled nuclei which is dependent on the choice of t_1 and t_2. The most striking signal loss of up to 78% of the total signal occurs with the symmetrical PRESS sequence ($t_1 = t_2$) at an echo time of $2/J$ ($\simeq$290 ms). Calculations have shown that this signal loss is related to the pulse angle distributions produced by the two refocusing pulses which leads to the creation of single quantum polarization transfer (PT) as well as to not directly observable states (NDOS) of the lactate AX_3 spin system: zero- and multiple-quantum coherences, and longitudinal spin orders. In addition, the chemical shift dependent voxel displacement (VOD) leads to further signal loss. By calculating the density operator for various of the echo times $TE = n/J, n = 1, 2, 3, \ldots$, we calculated quantitatively the contributions of these effects to the signal loss as well as their spatial distribution. A maximum signal loss of 75% can be expected from theory for the symmetrical PRESS sequence and $TE = 2/J$ for Hamming filtered sinc pulses, whereby 47% are due to the creation of NDOS and up to 28% arise from PT. Taking also the VOD effect into account (2 mT/m slice selection gradients, 20-mm slices) leads to 54% signal loss from NDOS and up to 24% from PT, leading to a maximum signal loss of 78%. Using RE-BURP pulses with their more rectangular pulse angle distributions reduces the maximum signal loss to 44%. Experiments at 1.5 T using a lactate solution demonstrated a maximum lactate signal loss for sinc pulses of 82% (52% NDOS, 30% PT) at TE = 290 ms using the symmetrical PRESS sequence. The great signal loss and its spatial distribution is of importance for investigations using a symmetrical PRESS sequence at $TE = 2/J$.

Key Words: **localized ^{1}H NMR spectroscopy; lactate; PRESS.**

INTRODUCTION

Single voxel localized proton spectroscopy is frequently performed using point-resolved spectroscopy (PRESS), a $90^\circ - 180^\circ - 180^\circ -$ Acq. double spin echo pulse train. The three slice selective pulses are successively applied to select a single voxel. In early work the PRESS method was used as a

$$90^\circ - t - 180^\circ - 2t - 180^\circ - t - \text{Acq.} \qquad \text{[P1]}$$

pulse train with a total echo time of $TE = 4t$ (*1, 2)*. But soon a more general pulse train

$$90^\circ - t_1 - 180^\circ - t_1 + t_2 - 180^\circ - t_2 - \text{Acq.} \qquad \text{[P2]}$$

was introduced (*3–6*), together with theoretical (*3, 4, 6–9*) and experimental (*3–9*) descriptions of signal losses which occur for coupled homonuclear spin systems compared to uncoupled spins. Here the total echo time is defined as $TE = TE_1 + TE_2 = 2t_1 + 2t_2$. For the lactate doublet, signal losses of more than 60% have been reported dependent on the time intervals t_1 and t_2 used (*3, 4, 6–9*). Three effects compete for the responsibility for the signal loss. The first two effects arise from the pulse angle distributions produced by the two slice selective refocusing pulses: first, the creation of not directly observable states (NDOS) of the lactate spin system, namely zero- and multiple-quantum coherences and longitudinal spin orders (*3, 6*), and second, the single quantum polarization transfer PT (*9*). The third effect is the chemical-shift-dependent voxel displacement VOD (*4, 7, 8*).

In spectroscopic investigations on lactate, usually echo times $TE = n/J$, $n = 1, 2, 3, \ldots$, are used to prevent phase anomalies of the lactate doublet. Thus, just these echo times were considered in this study. In practice, however, in most cases only the shorter echo times are useful, so a focus on $TE = 1/J$ and $2/J$ is to be desired. The VOD effect was found to predict no signal loss for $TE = 1/J$, but was made responsible for the signal loss at $2/J$ (*8*). Therefore, we examined in this study quantitatively the contributions and spatial distributions of the effects of NDOS, PT, and VOD with a special focus on $TE = 2/J$ ($\simeq$290 ms). This was performed by calculating and analyzing the quantum-mechanical density operator which makes it possible to describe the state of the spin system at the time of data acquisition, and experimentally at 1.5 T by using a solution of lactate and acetic acid in water. Unfavorable timing of the PRESS sequence around TE = 290 ms leads to a signal loss for the lactate doublet of 82%, in very good agreement with 78% predicted by the theory.

1090-7807/01 $35.00

THEORY

A schematic representation of the PRESS sequence for spatial localization is shown in Fig. 1. Ideally, the two refocusing pulses should be 180° pulses. However, a main drawback of these slice selective pulses and the whole PRESS sequence is, that the refocusing pulses themselves produce transverse magnetization (M_t) outside the centers of the slices; see Fig. 2. The amount and spatial distribution of the transverse magnetization depends on the pulses used and is given in Fig. 2 for the 2.56-ms Hamming-filtered sinc pulse, which excites a 20-mm slice using a 2 mT/m gradient, a pulse which is frequently used with PRESS spectroscopy. In addition, a Gaussian pulse which leads to an increased amount of transverse magnetization and a RE-BURP pulse (*10*) which shows less transverse magnetization are given. To guarantee high-quality localization the M_t components are eliminated by spoiler gradients applied within the PRESS sequence (see Fig. 1). However, despite the fact that the M_t components are eliminated due to the dephasing effect of the spoiler gradients, an important problem remains: the pulse angle decreases more or less rapidly to zero outside the centers of the slices. See Fig. 3, left column. This means, that a calculation of the PRESS sequence should take into account that the pulse angles vary over the slices and that gradients are applied according to Fig. 1. Therefore, the PRESS experiment which was used for calculation is represented by the pulse train for the symmetrical PRESS sequence and $\mathrm{TE} = 2n/J$, $n = 1, 2, 3, \ldots$,

$$\alpha_A^x \alpha_X^x - t - \beta_A^y \beta_X^y - 2t - \gamma_A^y \gamma_X^y - t - \mathrm{Acq.}, \qquad [P3]$$

and by

$$\alpha_A^x \alpha_X^x - t_1 - \beta_A^y \beta_X^y - t_1 + t_2 - \gamma_A^y \gamma_X^y - t_2 - \mathrm{Acq.}, \quad t_1 \ll 1/J, \qquad [P4]$$

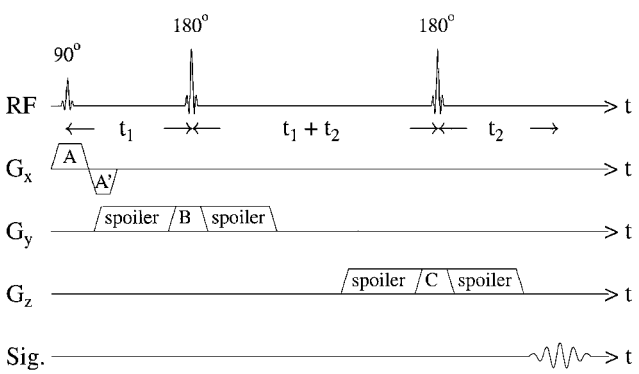

FIG. 1. The double spin echo sequence (PRESS) in a schematical representation. The slice selection gradients are given by A, A′, B, and C. Spoiler gradients are applied to guarantee high quality localization.

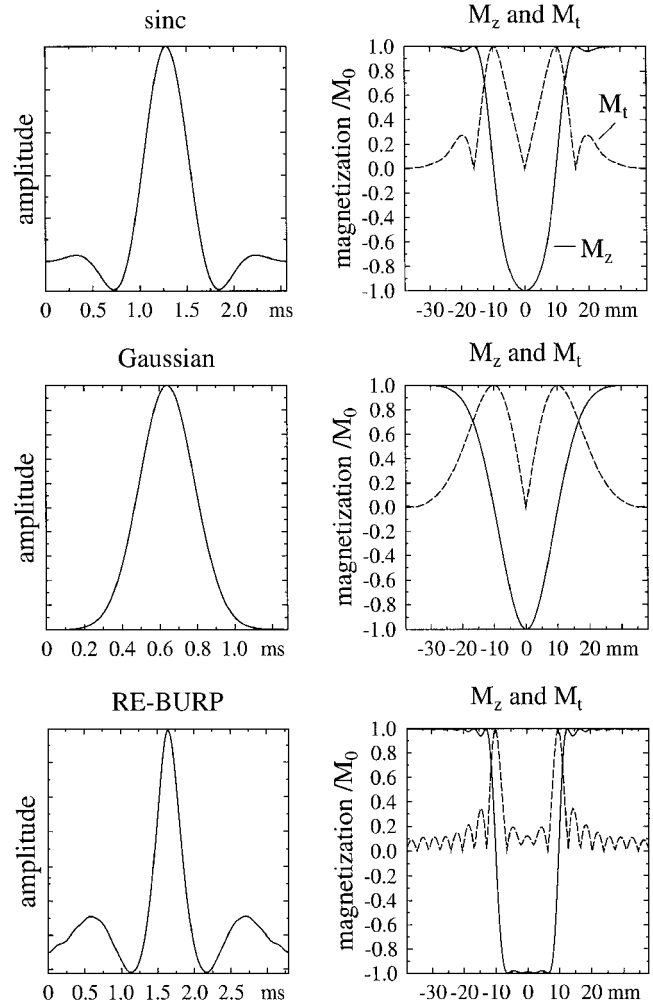

FIG. 2. Numerically determined longitudinal (M_z) and transverse (M_t) magnetization after application of different slice-selective 180° pulses with a bandwidth (FWHM) of 1704 Hz. These 180° pulses result in 20-mm slice thicknesses if they are applied in the presence of a 2 mT/m gradient. Top: 2.56 ms 180° Hamming-filtered sinc pulse; center: 1.28 ms 180° Gaussian pulse; bottom: 3.39 ms 174° RE-BURP pulse.

for the asymmetrical PRESS sequence and $\mathrm{TE} = n/J$, $n = 1, 2, 3, \ldots$. The symbol "α_A^x" represents an α pulse with phase x applied to the A-nucleus which serves for the excitation of a slice. Due to the chemical shift dependent displacement the same α pulse excites a spatially shifted slice for the three X-nuclei, which is represented by α_X^x. That means that the pulse angle α is different at most points within the voxel, as is also the case for β and γ (see, for example, Fig. 3, left column). In the following, the phase of the three pulses defined in [P3] and [P4] will no longer be given within calculations. The density operator for these PRESS experiments with the weakly coupled spin 1/2 systems can be calculated using the product operator formalism (*10*). Our calculations include the assumptions that the pulses are of infinitesimal short duration and that no relaxation occurs.

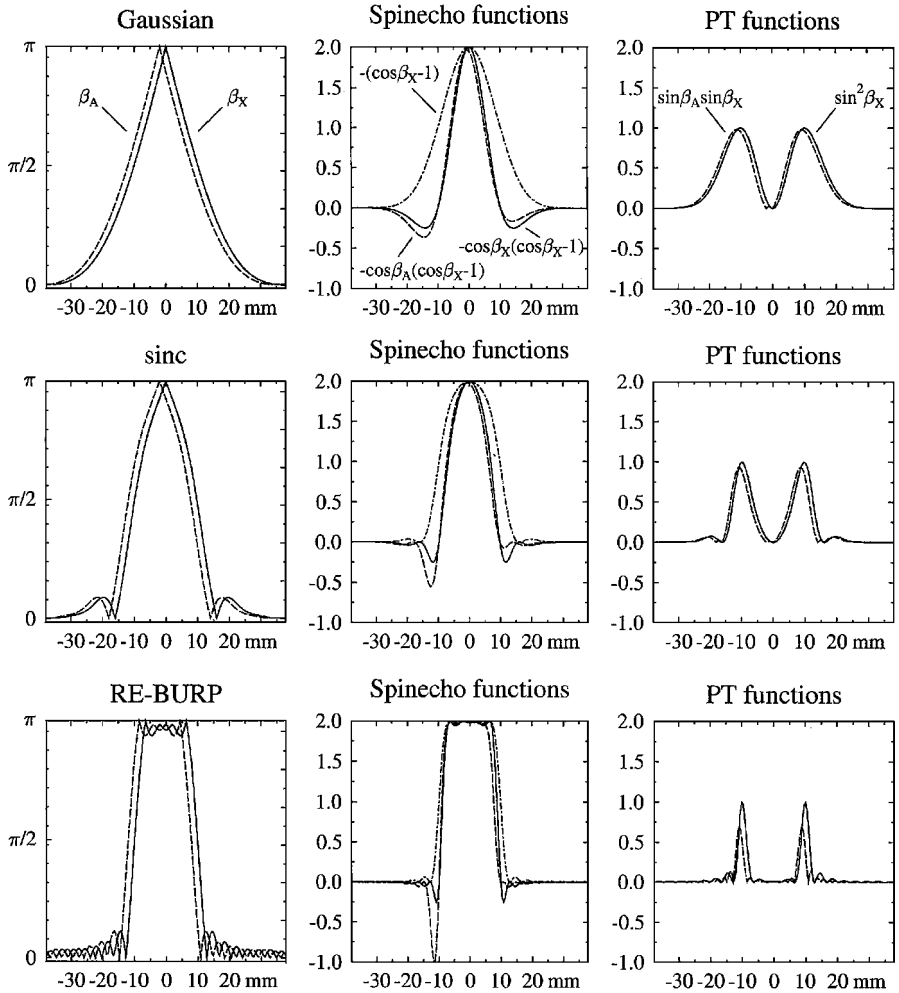

FIG. 3. Numerically determined pulse angle distributions (left column) in the direction of the slice selection gradient after slice-selective 180° pulses (dashed line: A-nucleus; solid line: X-nuclei). The pulse angle distribution in combination with the amplitudes of the normal spin echo of the X_3-nuclei in Table 1 leads to the spatial distribution presented in the central and right columns (dash–dotted line: uncoupled X-nucleus; solid line: X_3-nuclei without VOD effect; dashed line: X_3-nuclei with VOD effect). To be more easily comparable, the term (cos $\beta - 1$) which corresponds to the case of an uncoupled X-nucleus is also given but is negative, so that all functions show the value 1 in the center of the slice. The right column shows the corresponding spatial distribution of the double PT. Top: 2.56-ms 180° Hamming-filtered sinc pulse; center: 1.28-ms 180° Gaussian pulse; bottom: 3.39-ms 174° RE-BURP pulse. The RE-BURP pulse produces a pulse angle of 180° outside the center of the slice if a nominal pulse angle of 174° is used in the center of the slice.

For an uncoupled X spin system the density operator at the time of data acquisition in the PRESS sequence is

$$\sigma(\text{Acq.}) = -0.25 I_y \sin(\alpha_X)(\cos(\beta_X) - 1)(\cos(\gamma_X) - 1) \quad [1]$$

independent of the question whether the symmetrical sequence [P3] or the asymmetrical sequence [P4] is applied and independent of the echo time used.

A similar calculation of the density operator for the weakly coupled AX_3 spin system of lactate with variable t_1 and t_2 was not possible, because this leads to an explosion in the number of terms obtained. However, in spectroscopic investigations on lactate usually echo times $\text{TE} = n/J$, $n = 1, 2, 3, \ldots$, are used to prevent phase anomalies of the lactate doublet. Thus, just these echo times will be considered in the following, namely $\text{TE} = 4t = 2n/J$, $n = 1, 2, 3, \ldots$, for the symmetrical PRESS sequence [P3] and echo times $\text{TE} = n/J$, $n = 1, 2, 3, \ldots$, for the asymmetrical PRESS sequence [P4].

The Symmetrical PRESS Sequence [P3] at $TE = 4t = 2n/J$, $n = 1, 2, 3, \ldots$

With the assumptions made, the density operator for the AX_3 spin system can be calculated using the symmetrical PRESS sequence. For the case of $\text{TE} = 4t = 4/J, 8/J, 12/J, \ldots$ the solution for the pulse train [P3] can be easily calculated because in this case both refocusing pulses are applied at times when no antiphase magnetization is present. Thus, the coupled spin system behaves like an uncoupled system and we obtain for the

A-nucleus and the three X-nuclei (compare with Eq. [1])

$$\sigma(\text{Acq.}) = -0.25 I_{1y} \sin(\alpha_A)(\cos(\beta_A) - 1)(\cos(\gamma_A) - 1) - 0.25\left(I_{2y} + I_{3y} + I_{4y}\right) \sin(\alpha_X) \times (\cos(\beta_X) - 1)(\cos(\gamma_X) - 1). \quad [2]$$

I_1 is the A-spin and I_2, I_3, and I_4 are the three X-spins.

Using the symmetrical PRESS sequence and echo times $\text{TE} = 4t = 2/J, 6/J, 10/J, \ldots$, the density operator is more complex:

$$\begin{aligned}\sigma(\text{Acq.}) = {} & + \sin(\alpha_A)[-0.25 I_{1y} \cos^3(\beta_X)(\cos(\beta_A) - 1)\cos^3 \\ & \times (\gamma_X)(\cos(\gamma_A) - 1) - I_{1y}(I_{2z} I_{3z} + I_{2z} I_{4z} + I_{3z} I_{4z}) \\ & \times \sin(\beta_A)\sin(\beta_X)\cos(\gamma_X)(\cos(\gamma_A) - 1)\cos(\delta t) \\ & - I_{1y}(I_{2z} I_{3z} + I_{2z} I_{4z} + I_{3z} I_{4z})\cos(\beta_A)(\cos(\beta_X) - 1) \\ & \times \sin(\gamma_A)\sin(\gamma_X)\cos(\delta t) + I_{1x}(I_{2z} I_{3z} + I_{2z} I_{4z} \\ & + I_{3z} I_{4z})\sin(\beta_A)\sin(\beta_X)\cos(\gamma_X)(\cos(\gamma_A) - 1) \\ & \times \sin(\delta t) - I_{1x}(I_{2z} I_{3z} + I_{2z} I_{4z} + I_{3z} I_{4z})\cos(\beta_A) \\ & \times (\cos(\beta_X) - 1)\sin(\gamma_A)\sin(\gamma_X)\sin(\delta t) - 0.75 I_{1y} \\ & \times \sin(\beta_A)\sin(\beta_X)\cos^2(\beta_X)\sin(\gamma_A)\sin(\gamma_X) \\ & \times \cos^2(\gamma_X)\cos(2\delta t) - 0.75 I_{1x}\sin(\beta_A)\sin(\beta_X) \\ & \times \cos^2(\beta_X)\sin(\gamma_A)\sin(\gamma_X)\cos^2(\gamma_X)\sin(2\delta t)] \\ & + \sin(\alpha_X)[-0.25(I_{2y} + I_{3y} + I_{4y})\cos(\beta_A) \\ & \times (\cos(\beta_X) - 1)\cos(\gamma_A)(\cos(\gamma_X) - 1) - 0.25 \\ & \times (I_{2y} + I_{3y} + I_{4y})\sin(\beta_A)\sin(\beta_X)\sin(\gamma_A) \\ & \times \sin(\gamma_X)\cos(2\delta t) + 0.25(I_{2x} + I_{3x} + I_{4x}) \\ & \times \sin(\beta_A)\sin(\beta_X)\sin(\gamma_A)\sin(\gamma_X)\sin(2\delta t)]. \quad [3]\end{aligned}$$

The density operator in Eq. [3] contains only terms that lead to an observable signal. δ is the Larmor frequency difference between the two coupling partners. The last three lines of Eq. [3] contain magnetizations which belong to the three X-spins while all other terms contain A-spin magnetizations. The terms for the three X-spins are identical to those presented previously by Marshall and Wild (*12*).

The application of [P3] with $\text{TE} = 4t = 2/J, 6/J, 10/J, \ldots$ results in the creation of NDOS by the two refocusing pulses β and γ. These states of the spin system produced by β cannot result in observable magnetization unless they are transferred back to single quantum coherences (SQC) by the second refocusing pulse γ. However, in the PRESS sequence even a transfer of NDOS back to SQC does not give rise to a signal because these SQC are dephased by the spoiler gradients applied within the PRESS sequence; see Fig. 1 (*6*). Also, NDOS produced by γ do not give rise to observable signals. Consequently, NDOS terms do not occur in Eq. [3], however, their excitation leads to changes in the observable terms therein, leading to a signal loss as will be shown below. Thus, PRESS is a sequence which limits detection to coherences which remain single quantum coherences throughout the entire sequence. Among the observable terms a further effect occurs which can lead to a signal loss and which is also restricted to a coupled spin system: the single-quantum polarization transfer PT (*9*). PT occurs also during the transmission of the β- and γ-pulses, but in contrast to the NDOS, the PT terms remain single quantum coherences throughout the PRESS sequence. The PT terms show a dependence on δ, in contrast to the SQC of the normal spin echo.

It is interesting that the application of the symmetrical PRESS sequence [P3] and $\text{TE} = 4t = 4/J, 8/J, 12/J, \ldots$ produces neither MQC or ZQC nor PT, thus no signal loss has to be expected. The latter is in agreement with Yablonski *et al.* (*8*) who defined the echo time $\text{TE} = 4/J$ as "magic echo time". No dependence on the timing of the sequence exists in Eq. [2] and no VOD has to be taken into account, only a dependence on the pulse angles occurs. Of course, in Eq. [2] the origin of the signal from the A-nucleus is also spatially shifted in three dimensions with respect to the origin of the signal from the three X-nuclei; however, their signal intensity is not dependent on the size of this shift in Eq. [2], in contrast to Eq. [3], as will be shown with the following analysis.

Normal spin–echo terms. The trigonometric terms in Eq. [3] corresponding to the normal spin–echo for the A-nucleus have the form $\cos^3(\beta_X)(\cos(\beta_A) - 1)\cos^3(\gamma_X)\ (\cos(\gamma_A) - 1)$, while for the three X-nuclei the form is $\cos(\beta_A)(\cos(\beta_X) - 1)\cos(\gamma_A)\ (\cos(\gamma_X) - 1)$. These functions show considerable differences from the uncoupled X spin system, where the normal spin–echo shows the trigonometric behavior $(\cos(\beta_X) - 1)(\cos(\gamma_X) - 1)$; see Eq. [1]. These differences contribute to the signal loss observed for the lactate spin–echo signals.

The interrelationship between pulse angle distribution and spin system can be visualized best by calculating the pulse angle distribution from M_z and M_t of Fig. 2 using the equation

$$\beta = \frac{\pi}{2} - \arctan\left(\frac{M_z}{M_t}\right). \quad [4]$$

The results for all three pulse types used in Fig. 2 are shown in Fig. 3, left column, taking a chemical-shift-dependent slice displacement of 2 mm into account which is obtained for lactate with the 2 mT/m gradients used. Using these pulse angle distributions the spatial distributions of the normal spin–echo terms shown in Fig. 3, middle column, were calculated for the X_3 nuclei in Eq. [3] (dashed line) and the uncoupled X-nucleus in Eq. [1] (dash-pointed line). In addition, the normal spin–echo term for the X_3-nuclei is provided for the case with zero chemical shift displacement (solid line). The double PT terms of the X_3-nuclei in Eq. [3] could also be derived; see Fig. 3, right column. Again, distributions without taking the

chemical-shift-dependent displacement into account (solid line) are also provided.

Terms of single quantum polarization transfer PT. The density operator in Eq. [3] contains terms which depend on the difference of the Larmor frequencies $\delta = \Omega_2 - \Omega_1$ between the A-nucleus (Ω_1) and the X_3-nuclei (Ω_2). There are terms of nucleus A which contain a single PT produced by the β pulse and a normal spin echo hereafter represented by $\sin(\beta_A)\sin(\beta_X)\cos(\gamma_X)(\cos(\gamma_A)-1)$ and those produced after a normal spin echo by the γ pulse $\cos(\beta_A)(\cos(\beta_X)-1)\sin(\gamma_A)\sin(\gamma_X)$. These single PT terms oscillate with $\cos(\delta t)$ or $\sin(\delta t)$. No single PT terms occur for the three X-nuclei. Besides the single PT, the double PT also occurs; this means a PT which takes place at the β pulse and is reversed at the γ pulse. These terms show an oscillation with the frequency $\cos(2\delta t)$ or $\sin(2\delta t)$ and have a trigonometric dependence of $\sin(\beta_A)\sin(\beta_X)\cos^2(\beta_X)\sin(\gamma_A)\sin(\gamma_X)\cos^2(\gamma_X)$ for nucleus A and $\sin(\beta_A)\sin(\beta_X)\sin(\gamma_A)\sin(\gamma_X)$ for the three X-nuclei. We have previously discussed the density operator of the three X-nuclei and its creation via the double PT in more detail (*9*). These considerations showed that small deviations in the echo time from $2/J$ lead to phase and intensity distortion of the doublet signal of lactate by the signal contribution originating from double PT. A complete period of the double PT term is obtained at 1.5 T by the $\sin(2\delta t)$ and $\cos(2\delta t)$-dependence after 10.87 ms for the δ of $2\pi \cdot 184$ s^{-1} for lactate in the solution used.

Antiphase terms. The density operator of Eq. [3] contains terms of antiphase magnetization for the A-nucleus represented for example by $I_{1y}I_{2z}I_{3z}$, the antiphase y-magnetization of nucleus A with respect to nuclei 2 and 3 of the three X-nuclei. Such antiphase terms lead to phase and intensity anomalies of the lactate quartet. This result is exciting because usually one would expect pure inphase magnetization for $\mathrm{TE} = n/J$, $n = 1, 2, 3, \ldots$, in a conventional spin–echo sequence. However, this fact may easily be understood by an example: Inphase magnetization of the X_3-nuclei is present after the α pulse and is transferred to pure antiphase magnetization of the X_3-nuclei at the time where the β pulse is applied (TE/4) due to the J-coupling to the single A-nucleus. This antiphase magnetization is partially transferred by the β pulse from the X_3-nuclei to the A-nucleus. Thus, after the β pulse a new antiphase magnetization of the A-nucleus is created which develops after the β pulse for a period of 3TE/4 under the coupling to all three X-nuclei if not transferred back again by the γ pulse, that means, if the γ pulse produces a normal spin echo of this magnetization (see also above: "terms of single quantum polarization transfer"). The result is an antiphase magnetization of the A-nucleus at the time of data acquisition.

Spatial distribution. The signal intensity distribution within the volume element produced by two 2.56-ms Hamming-filtered sinc pulses (see Fig. 2) is plotted in Fig. 4a without and in Fig. 4b with VOD effect. Both figures show the spatial distribution of the intensities in the twodimensional space spanned by the spatial directions of the two refocusing pulses: the terms of an uncoupled X-system (top left) as well as the terms of the X_3-nuclei, the normal spin-echo term (top right), the double PT term (center right), and the addition of both terms (center left). The double PT effect is maximum at the corners where both refocusing pulses produce 90° pulse angles (center right). Dependent on its phase, the double. PT contribution can add constructively (center left) to the spin–echo term and by this to the total signal, or subtractively (not shown). The difference between the graph center left and top left is given on bottom left. Since the double PT is constructive in this example, this plot represents the spatial distribution of the signal loss which arises due to the creation of NDOS in the X_3-system compared to an uncoupled X-system. The spatial distribution of the signal loss of the lactate doublet (bottom left) is confined to the edges. No signal loss occurs in the center, where the pulse angle of both refocusing pulses is 180°.

A comparison of Figs. 4a and 4b shows that the VOD effect leads to small corrections of the results obtained without VOD.

Signal intensity. To determine the total signal intensity for lactate, the different terms containing the pulse angles in Eqs. [2] and [3] had to be integrated numerically over the volume element assuming constant lactate concentration over the sample. The corresponding results are given in Table 1. The terms $\sin(\alpha_A)$ and $\sin(\alpha_X)$ are factors which are identical for all terms. Thus, the integration could be carried out as a two-dimensional integration in the direction of the two refocusing pulses. We assumed, furthermore, that both refocusing pulses had an identical pulse angle distribution which should be given in practice if two identical pulses are used. The integral for the uncoupled X-system is given by the term $(\cos(\beta_X)-1)(\cos(\gamma_X)-1)$, which is used as a reference for the Hamming-filtered sinc pulse and set equal to 1. This represents the maximum signal intensity which can be obtained with the sinc pulses used.

The expected signal intensities for the lactate doublet can be calculated from Table 1. As a rule of thumb, Gaussian pulses produce a smaller and RE-BURP pulses a greater signal of the normal spin–echo. Vice versa, the greater contribution from PT occurs for Gaussian pulses while the RE-BURP pulse produces less PT. It is interesting that, with an uncoupled system, the Gaussian pulses produce 24% more signal and the RE-BURP pulses 8% more signal, compared to the sinc pulses. This is due to the broad wings of the $-(\cos\beta_X - 1)$ function for the Gaussian pulses, which lead to strong signal contributions from outside the halfwidth of the slice (see Fig. 3). For the RE-BURP pulse a more rectangular function is responsible for a signal gain achieved mainly within the halfwidth of the slice. For practical applications sinc pulses have frequently been used as a compromise between a superior slice profile compared to the Gaussian pulses and smaller transverse magnetization components far outside the slice compared to the RE-BURP pulses.

For the X_3-nuclei of lactate we can calculate the maximum signal intensity using Table 1: for sinc pulses the result is $0.34 + 0.12 = 0.46$ for $\cos(2\delta t) = 1$, for the case in which the double PT

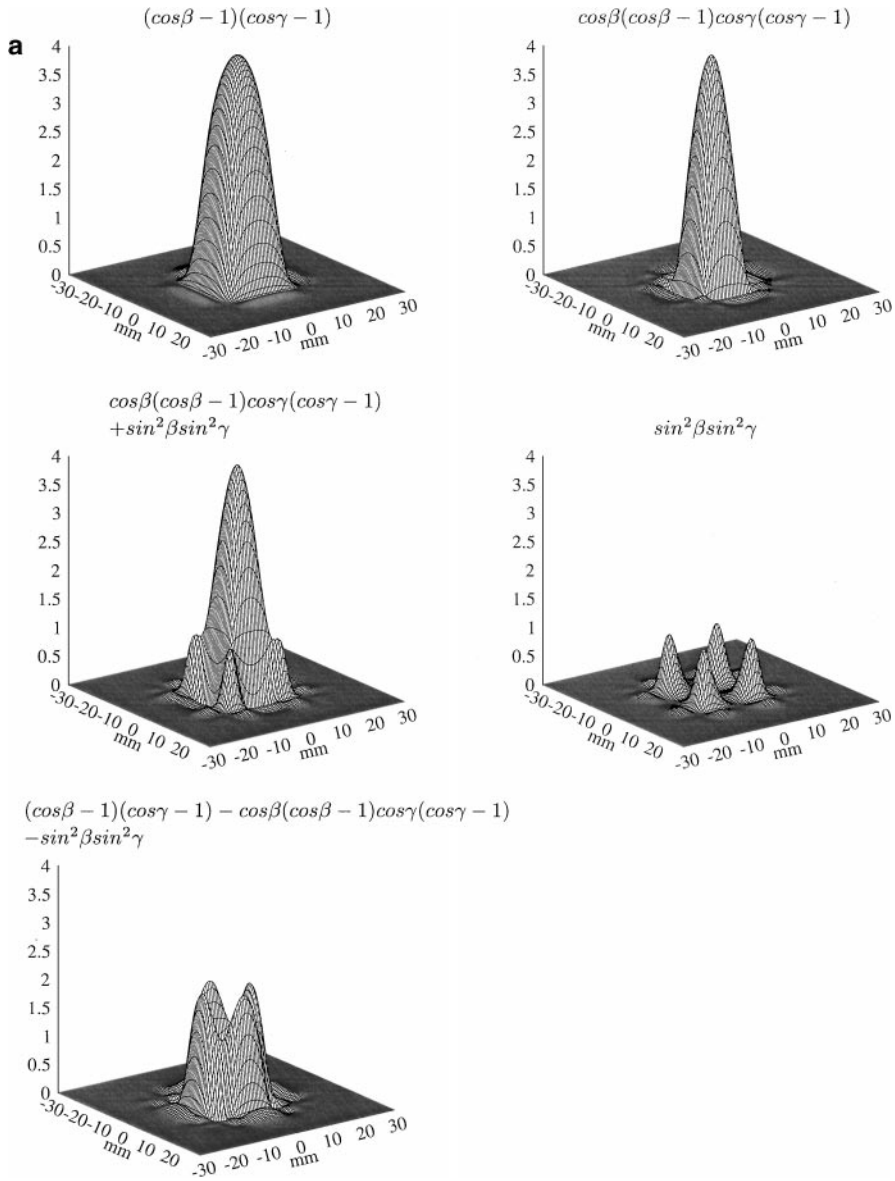

FIG. 4. Spatial distribution of the terms of the X_3-nuclei (see Eq. [3]) of lactate and the X-nucleus of an uncoupled spin system in Eq. [2]. Presented is the numerical result obtained with 2.56-ms Hamming-filtered 180° sinc pulses (halfwidth 1704 Hz corresponding to 20-mm slice thickness at 2 mT/m slice selection gradients): (a) without VOD effect; (b) with VOD effect. Top left: normal spin echo of an uncoupled spin system. Top right: normal spin echo term of the X_3-nuclei. Center left: addition of the normal spin echo and the positive double PT term of the X_3-nuclei. Center right: positive double PT term of the X_3-nuclei. Bottom left: difference between top left and center left representing the signal loss for the X_3-nuclei due to the creation of NDOS compared to uncoupled-nuclei.

adds constructively to the normal spin echo. The signal minimum of 0.22 is obtained for $\cos(2\delta t) = -1$ or a destructive addition. That means a lactate doublet signal loss between 54 and 78% is expected relative to an uncoupled signal. Without taking the VOD effect into account, the maximum signal intensity for sinc pulses is $0.39 + 0.14 = 0.53$ and the minimum signal is 0.25; thus, without the VOD effect, a signal loss between 47% and 75% is expected. It has to be pointed out that the signal loss for constructive addition still is on the order of 50%. Responsible for this greatest contribution to total signal loss is the creation of NDOS.

Compared to sinc pulses, Gaussian pulses lead to threefold greater double PT terms which dominate the total signal intensity over the contribution of the normal spin echo.

Using RE-BURP pulses with their more rectangular pulse angle distribution compared to both Gaussian and sinc pulses, the maximum total signal loss for the lactate doublet is only 44% (relative to an uncoupled signal), almost completely independent of PT (see Table 1). Without taking the VOD effect into account, a signal loss of 33% remains. This demonstrates that the VOD effect is responsible for 3 of the 78% total maximum signal loss which arises for sinc pulses, and for 11 of the 44%

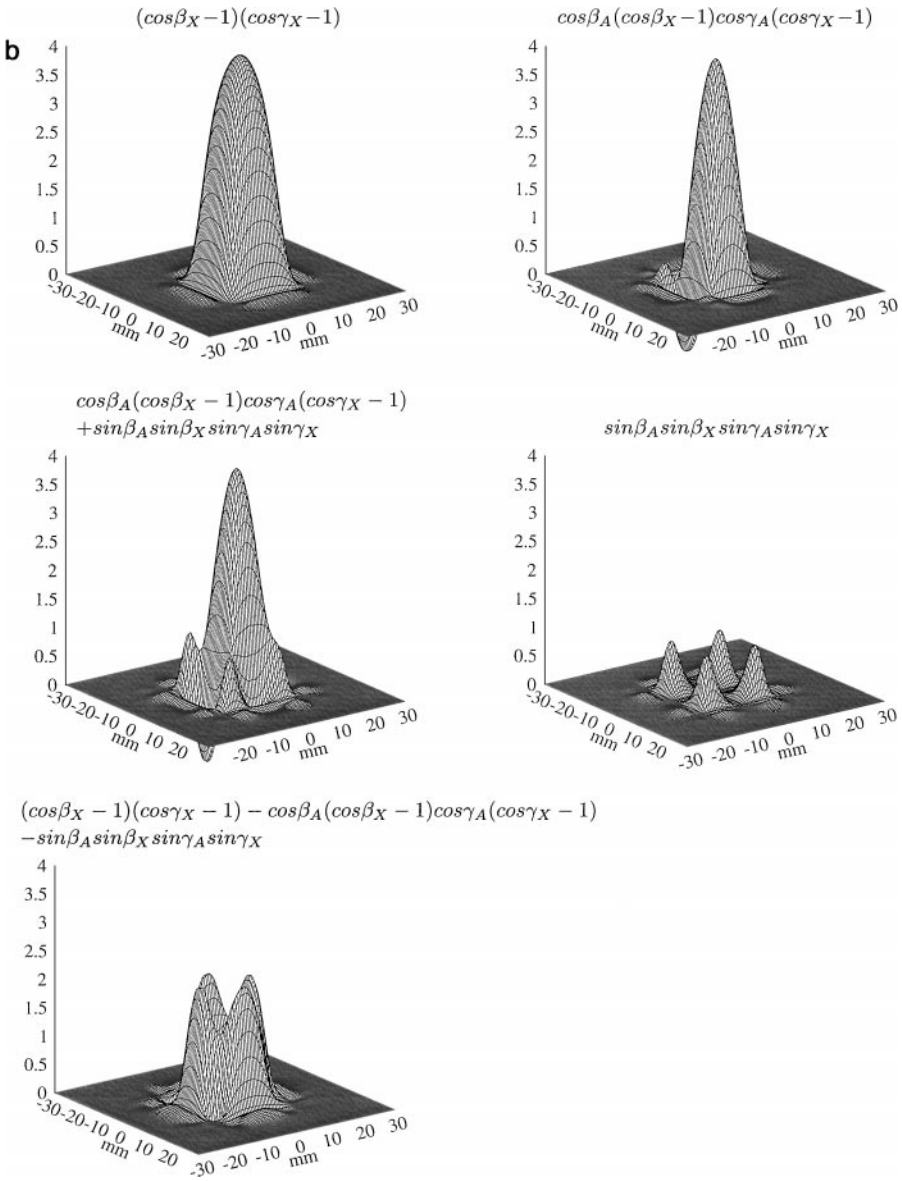

FIG. 4.—*Continued*

total maximum signal loss which arises using RE-BURP pulses. These relations are, however, only valid for the 2 mT/m slice selection gradients used for the calculations. Stronger gradients might be used to reduce the VOD effect; however, it should be kept in mind that also improved pulse angle distributions might then be obtained. Thus other gradient strengths demand their own calculations.

Finally, the signal intensity for the lactate quartet is mainly determined by the normal spin–echo term and by the single PT. Using sinc pulses, the terms of single PT are 20 times greater than the double PT terms (0.20 vs 0.01); therefore, the latter play a very secondary role. The antiphase x-terms cancel via spatial integration so that the antiphase y-terms and the normal spin echo term dominate the total signal of the A-nucleus. The superposition of both leads to the expectation of phase and intensity distortions for the quartet.

The Asymmetrical PRESS Sequence [P4] at $TE = n/J$, $n = 1, 2, 3, \ldots$

The asymmetrical sequence [P4] with an echo time of $TE = n/J$ is characterized by a t_1 interval which is kept as small as possible; thus the β pulse has to be applied as fast as technically possible after the α pulse. For the following calculations we assumed that the t_1 interval is so short that a spin–echo is produced by the β pulse, but that the antiphase terms are negligibly small; i.e., $t_1 \ll 1/J$ and $t_2 \simeq n/2J = TE/2$.

For the case of $n = 2, 4, \ldots$ the solution for pulse train [P4] can be easily calculated because in this case both refocusing pulses

TABLE 1
Numerically Integrated Signal Using Symmetrical PRESS

Symmetrical PRESS	sinc	Gaussian	RE-BURP
Normal spin echo			
X uncoupled: $(\cos(\beta_X)-1)(\cos(\gamma_X)-1)$	1.00	1.24	1.08
X_3-nuclei: $\cos(\beta_A)(\cos(\beta_X)-1)\cos(\gamma_A)(\cos(\gamma_X)-1)$			
with VOD	0.34	0.20	0.61
without VOD	0.39	0.22	0.75
A-nucleus: $\cos^3(\beta_X)(\cos(\beta_A)-1)(\cos^3(\gamma_X)(\cos(\gamma_A)-1)$			
with VOD	0.21	0.12	0.56
without VOD	0.24	0.13	0.66
Single PT			
A-nucleus: $\sin(\beta_A)\sin(\beta_X)\cos(\gamma_X)(\cos(\gamma_A)-1)$			
with VOD	0.20	0.28	0.09
without VOD	0.23	0.30	0.15
A-nucleus: $\cos(\beta_A)(\cos(\beta_X)-1)\sin(\gamma_A)\sin(\gamma_X)$			
with VOD	0.20	0.28	0.09
without VOD	0.23	0.30	0.15
Double PT			
X_3-nuclei: $\sin(\beta_A)\sin(\beta_X)\sin(\gamma_A)\sin(\gamma_X)$			
with VOD	0.12	0.39	0.01
without VOD	0.14	0.41	0.03
A-nucleus: $\sin(\beta_A)\sin(\beta_X)\cos^2(\beta_X)\sin(\gamma_A)\sin(\gamma_X)\cos^2(\gamma_X)$			
with VOD	0.01	0.03	0.00
without VOD	0.02	0.03	0.00

Note. Numerically determined integrals over the two spatial dimensions represented by the two refocusing pulses β and γ. The corresponding trigonometric terms of Eq. [3] are given, which are valid for the symmetrical PRESS sequence and TE $= 2/J, 6/J, 10/J \ldots$ In addition, the term for the spin echo of an uncoupled X-nucleus is also provided represented by $(\cos(\beta_X)-1)(\cos(\gamma_X)-1)$ and its integral was used to normalize the integral to 1 for the use of sinc pulses. This integral represents the maximum attainable signal for the given pulse angle distribution of the sinc pulse shown in Fig. 2, 20-mm slices, and 2 mT/m slice selection gradients. The values were determined for the pulse angle distributions shown in Fig. 3 and are only valid for these distributions.

are applied at times where only negligible antiphase magnetization is present. Thus, the coupled-spin system behaves like an uncoupled system and we obtain for the A-nucleus and the three X-nuclei

$$\begin{aligned}\sigma(\text{Acq.}) \simeq\ & -0.25 I_{1y}\sin(\alpha_A)(\cos(\beta_A)-1)(\cos(\gamma_A)-1)\\ & -0.25(I_{2y}+I_{3y}+I_{4y})\sin(\alpha_X)(\cos(\beta_X)-1)\\ & \times(\cos(\gamma_X)-1),\end{aligned} \quad [5]$$

which is for $t_1 \to 0$ identical to the results for the symmetrical sequence presented in Eq. [2].

For $n = 1, 3, 5 \ldots$ in pulse train [P4], more complex behavior exists because NDOS are excited by the γ pulses, which do not contribute to the total signal. The total density operator in this case is:

$$\begin{aligned}\sigma(\text{Acq.}) \simeq\ & -0.25 I_{1y}\sin(\alpha_A)(\cos(\beta_A)-1)(\cos(\gamma_A)-1)\\ & \times\cos^3(\gamma_X) - I_{1y}(I_{2z}I_{3z}+I_{2z}I_{4z}+I_{3z}I_{4z})\sin(\alpha_A)\\ & \times(\cos(\beta_X)-1)\sin(\gamma_A)\sin(\gamma_X)\cos(\delta t)\\ & - I_{1x}(I_{2z}I_{3z}+I_{2z}I_{4z}+I_{3z}I_{4z})\sin(\alpha_A)\\ & \times(\cos(\beta_X)-1)\sin(\gamma_A)\sin(\gamma_X)\sin(\delta t)\\ & - 0.25(I_{2y}+I_{3y}+I_{4y})\sin(\alpha_X)(\cos(\beta_X)-1)\\ & \times\cos(\gamma_A)(\cos(\gamma_X)-1).\end{aligned} \quad [6]$$

In contrast to the application of the symmetrical sequence which leads to the terms represented by Eq. [3], no terms of double PT occur in Eq. [6] because the only pulse which can create PT is the γ pulse.

Signal intensity using the asymmetrical sequence. To calculate the total signal intensity obtained with the asymmetrical sequence, again a two-dimensional numerical integration was carried out in the direction of the two refocusing pulses. The results are presented in Table 2 for all three pulses used in Fig. 2. As in Table 1, the normal spin–echo of an uncoupled X-system is used as a reference and given for comparison. It should be stated again that for TE $= 2/J, 4/J, \ldots$ Eq. [5] applies; that means that no lactate signal loss occurs for $t_1 \to 0$, and lactate behaves like an uncoupled spin system. For TE $= 1/J, 3/J, \ldots$ the asymmetrical sequence produces a signal intensity for lactate which is dependent on the pulse angle distributions of the refocusing pulses. For the X_3-nuclei of lactate and the use of sinc pulses, a signal intensity of 0.59 is obtained, or in other words, a signal loss of 41% has to be expected at echo times of TE $= 1/J, 3/J, \ldots$ while no signal loss occurs for TE $= 2/J, 4/J, \ldots$. If the VOD effect is not taken

TABLE 2
Numerically Integrated Signal Using Asymmetrical PRESS

Asymmetrical PRESS	sinc	Gaussian	RE-BURP
Normal spin echo			
X uncoupled: $(\cos(\beta_X)-1)(\cos(\gamma_X)-1)$	1.00	1.24	1.08
X_3-nuclei: $(\cos(\beta_X)-1)\cos(\gamma_A)(\cos(\gamma_X)-1)$			
with VOD	−0.59	−0.50	−0.81
without VOD	−0.62	−0.52	−0.90
A-nucleus: $(\cos(\beta_A)-1)\cos^3(\gamma_X)(\cos(\gamma_A)-1)$			
with VOD	−0.46	−0.38	−0.77
without VOD	−0.49	−0.40	−0.84
Single PT			
A-nucleus: $(\cos(\beta_x)-1)\sin(\gamma_A)\sin(\gamma_X)$			
with VOD	−0.35	−0.69	−0.12
without VOD	−0.38	−0.71	−0.18

Note. Numerically determined integrals over the two spatial dimensions represented by the two refocusing pulses β and γ. The corresponding trigonometric terms of Eq. [6] are given which are valid for the asymmetrical PRESS sequence and TE $= 1/J, 3/J, 5/J$... In addition, the term for the spin echo of an uncoupled X-nucleus is also provided represented by $(\cos(\beta_X)-1)(\cos(\gamma_X)-1)$ and its integral was used to normalize the integral to 1 for the use of sinc pulses. This integral represents the maximum attainable signal for the given pulse angle distribution of the sinc pulse shown in Fig. 2, 20-mm slices, and 2 mT/m slice selection gradients. The values were determined for the pulse angle distributions shown in Fig. 3 and are only valid for these distributions.

into account the signal loss decreases by 3 to 38% in total. The signal losses for Gaussian pulses are greater with 60% and 58% (with and without VOD), while smaller signal losses of 25% and 17%, respectively, occur for RE-BURP pulses. It is obvious that the contribution of the VOD effect to the total signal loss of the lactate doublet increases for more rectangular pulse angle distributions: while the VOD leads to 2% greater signal loss for Gaussian pulses, it increases by 8% for RE-BURP pulses.

It should be noted that no PT terms exist for the X_3-nuclei, so that no phase anomalies occur, in contrast to the use of the symmetrical PRESS sequence.

Finally, it is interesting to focus on the situation which can arise in practice: If the echo time $2/J$ is desired, the symmetrical sequence leads to a signal loss of up to 78% for sinc pulses, while the asymmetrical sequence works without signal loss.

MATERIALS AND METHODS

Experimental data were obtained on a Siemens 1.5 T SP63 whole-body imager (Siemens Medizintechnik, Erlangen, Germany) using the standard circularly polarized head coil. A glass sphere (500 ml) filled with a solution of Ca lactate (100 mMol/L) and acetic acid (400 mMol/L) in water was positioned in the center of the coil. The Larmor frequency difference δ between the quartet and the doublet of lactate was determined to $2\pi \cdot 184\,\mathrm{s}^{-1}$ at 1.5 T.

The PRESS sequence schematically shown in Fig. 1 was used in combination with water suppression by a 35.84-ms frequency-selective saturation pulse followed by a spoiler gradient (not shown). Since the bandwidth of this pulse was only 70 Hz, no influence of the water elimination process on the observed spectral components was found. To guarantee a proper localization spoiler gradients were applied before and after the slice selection gradients B and C of the two 180° pulses.

The symmetrical and asymmetrical PRESS sequences were used with echo times (TE) of 288, 290 ($2/J$), and 293 ms to select $2 \times 2 \times 2$ cm voxels. For slice selection (bandwidth = 1704 Hz), 2.56 ms Hamming-filtered sinc pulses were used in combination with 2 mT/m gradients. The pulse angles were inline adjusted using a procedure provided by the manufacturer.

The signals were acquired fully relaxed with 2K data points and one acquisition, multiplied by a Gaussian function ($t_{1/2} = 500$ ms, $t_0 = 0$ ms), zerofilled to 4K, Fourier transformed and zero-order phase-corrected until a pure absorption mode acetic acid singulet was obtained. No higher order phase correction and no baseline correction was applied. This led to the spectra in Fig. 5. From these spectra the signal integrals were determined and the integral ratio R of the lactate doublet to the acetic acid singlet was calculated. For the phase-distorted doublet at TE = 290 ms in Fig. 5 central and bottom row an additional phase correction was applied to obtain pure absorption mode signals prior to integration.

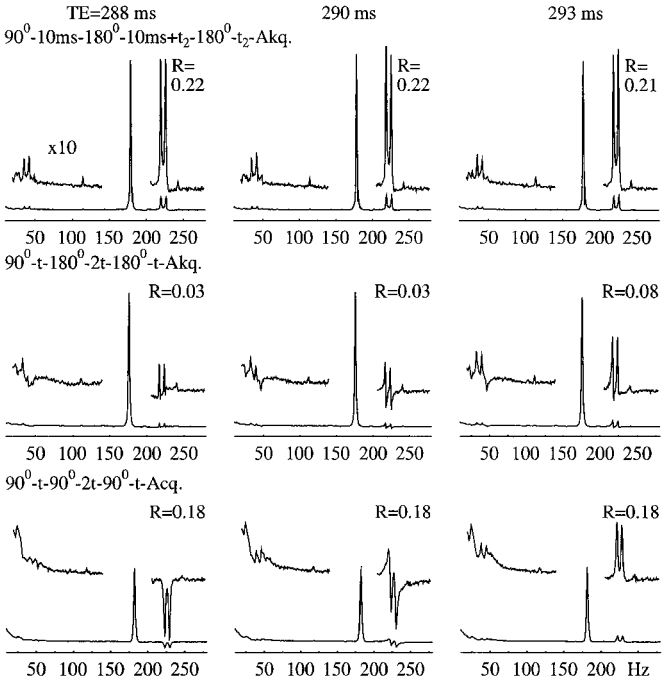

FIG. 5. Localized ^{1}H PRESS spectra of a lactate and acetic acid solution obtained with different PRESS sequences. Top row: $90° - 10\,\mathrm{ms} - 180° - 10\,\mathrm{ms} + t_2 - 180° - t_2 -$ Acq. Central row: $90° - t - 180° - 2t - 180° - t -$ Acq. Bottom row: $90° - t - 90° - 2t - 90° - t -$ Acq. The asymmetrical PRESS sequence (top row) leads to a negligible signal loss for the lactate doublet while the symmetrical sequence (central row) results in a signal loss between 86% (TE = 288 ms) and 62% (TE = 293 ms). This variation in the signal loss is dependent on the double PT. The double PT effect is visible best if 90° refocusing pulses are used (bottom row) because this leads to maximum double PT. The double PT contributions are subtractive at TE = 288 ms, additive at TE = 293 ms, and out of phase at TE = 290 ms ($2/J$). These spectra give an impression of the phase behavior of the (smaller) double PT contributions to the spectra in the central row obtained with 180° refocusing pulses. Data: $\delta = 2\pi 184$/s, $2 \times 2 \times 2$ cm voxels, 1 acquisition, 2K data points, 4K zerofill, Gaussian filter with $t_{1/2} = 500$ ms, spectral width ±500 Hz, zero order phase correction until a pure absorption mode acetic acid singulet was obtained.

EXPERIMENTAL RESULTS

Figure 5 shows the spectra obtained from the lactate and acetic acid solution with the asymmetrical PRESS sequence ($t_1 = 10$ ms, top row), the symmetrical PRESS sequence (central row), and the symmetrical PRESS sequence with 90° refocusing pulses ($90° - t - 90° - 2t - 90° -$ Acq., bottom row) and echo times of 288, 290, and 293 ms. The echo time of 290 ms corresponds to $2/J$ (*6*). The acetic acid signals showed similar signal intensities irrespective of the timing of the sequence. In contrast, the signal intensity of the lactate doublet obtained with the symmetrical sequence was drastically reduced. The lactate doublet to acetic acid singlet ratio R is given for each spectrum by the number plotted close to the doublet. R was reduced to values between 38% (TE = 293 ms) and 14% (TE = 288 ms) compared with the asymmetrical sequence. This is the major effect observed. A minor effect was obtained with a variation of

the echo time. This led to negligibly small changes for the lactate signals if the asymmetrical sequence was used but produced moderate changes using the symmetrical PRESS sequence, as expected from the double PT contributions. The double PT terms show a sinusoidal change of their phase with a frequency of $\delta/2$ (*9*). This fact is best visible if 90° refocusing pulses are used (bottom row), because this leads to maximum double PT and to zero spin–echo signal (see Eq. [3]). The corresponding spectra give an impression of the phase behavior of the (smaller) double PT contributions to the spectra in the central row obtained with 180° refocusing pulses: The double PT contributions are subtractive at TE = 288 ms, additive at TE = 293 ms, and out of phase at TE = 290 ms ($2/J$). δ corresponded to $2\pi \cdot 184\,s^{-1}$ at the 1.5-T field strength used, leading to a period of 10.86 ms. It has to be pointed out here that despite using 90° refocusing pulses the sequence remains a double spin–echo sequence and that a stimulated echo signal is prevented via the gradients used, see Fig. 1. The lactate doublet to acetic acid ratio R is identical for all bottom row spectra if the phase of the doublet is corrected to pure absorption mode prior to integration.

The measurements which led to the spectra in Fig. 5, central row, were repeated after 15 days with a slightly different result: The transmitter voltage for the 180° refocusing pulses as determined by the manufacturers inline adjustment procedure was 73.9 V (day 1) and 71.1 V (day 16). The corresponding lactate doublet to acetic acid ratios R also showed clear differences: the lactate doublet signal loss was between 62 and 86% for the first measurement, while the repeated measurement led to values between 52 and 82% (spectra not shown).

The lactate quartet is free of phase anomalies if the asymmetrical sequence is used at TE = $2/J$; see Fig. 5, top row. If the symmetrical PRESS sequence is used the quartet shows strong phase and intensity anomalies, as is obvious from the fact that the outer lines of the quartet are negative.

DISCUSSION

Theoretical calculations in this work revealed a signal loss by the lactate doublet compared with an uncoupled signal between 54 and 78% at an echo time of $2/J, 6/J, \ldots$ using the symmetrical PRESS sequence, 2.56-ms Hamming-filtered sinc pulses, and 2 mT/m gradients. Of the loss, 54% arises from the creation of NDOS while up to 24% can occur in addition due to the double PT.

The signal loss of the lactate doublet determined experimentally from the spectra in Fig. 5 is with values 62% (double PT constructive) and 86% greater than the values of 54 and 78% expected from theory. However, a repeated measurement with identical experimental circumstances caried out 15 days later showed smaller signal losses of 52% (double PT constructive) and 82% very close to the theoretical values. The difference between both measurements was that separate transmitter adjustments were carried out for both measurements. The transmitter voltage for the 180° refocusing pulses was 3.9% greater for the first measurement, reflecting that the signal loss is also dependent on the pulse angle calibration. This fact is not surprising because compared to an uncoupled system, the signal intensity for the AX_3 system is much more susceptible to deviations of the refocusing pulse angles from 180° (see also Figs. 3 and 4).

The great lactate doublet signal loss arises from three effects. First, the creation of NDOS leads to a signal loss in the outer regions of both directions defined by the gradients of the two refocusing pulses. This results in a signal reduction for the normal spin echo term. The resulting spatial distribution of the normal spin–echo term in Fig. 4b, top right shows no signal loss in the center but due to the signal loss at the edges a much narrower shape compared with the uncoupled spin system in Fig. 4b, top left. Second, the double PT effect occurs at the corners of the two-dimensional space. The double PT is maximum where both refocusing pulses produce 90° pulse angles, see Fig. 4b center right. Dependent on its phase, the double PT contribution can add constructively to the total signal, see Fig. 4b center left, or subtractively leading to an additional signal loss (not shown). Figure 4b bottom left shows the spatial distribution of the lactate signal loss for constructive contribution of the double PT term; that is, the signal loss that arises due to the creation of NDOS is shown. The fact that the signal loss occurs in the outer regions of the volume element is important for practical applications using the symmetrical PRESS sequence at TE = $2/J$: the lactate-containing structure should be positioned within the center of the volume element to prevent false negative results. Third, the VOD effect has to be taken into account, the effects of which lead to slight changes in intensity and spatial distribution of the signal of the lactate doublet as can be derived from Figs. 3 and 4 and Tables 1 and 2. All three effects as well as their spatial distributions could be analyzed individually with use of the theoretical considerations presented here. Using a numerical simulation, Thompson and Allen recently have also demonstrated a pulse angle dependence of the lactate signals (*13*). However, the paper provides overall signal intensities rather than separating the contributions and spatial dependence of the three individual effects and their corresponding signal loss.

One solution to the first two effects, the creation of NDOS and the double PT is to use superior refocusing pulses. Such pulses produce a pulse angle distribution which shows a more rectangular function; see Fig. 3. However, care has to be taken because transverse magnetization components may arise far outside the centers of the slices as, for example, if RE-BURP pulses are used. On the other hand it is possible to drastically reduce the signal loss for the symmetrical PRESS sequence to values between 33 and 44% using RE-BURP pulses, making the signal intensity also less susceptible to the PT effects. However, while the total signal loss decreases with the use of such pulses, the loss due to the VOD effect generally increases; see Tables 1 and 2. Moreover, it should be pointed out that pulses which produce a rectangular pulse angle distribution cannot be realized.

A further solution to the problem is the use of the asymmetrical PRESS sequence, which in theory ($t_1 \rightarrow 0$) produces no signal loss at a TE of $2/J$. However, to build up such a sequence

is impossible. An experimental approach is very demanding for the hardware components used because the first refocusing pulse has to be applied extremely fast after the 90° excitation pulse. Due to the finite pulse lengths and limitations in gradient rise time and strength it seems to be impossible to built up a perfect asymmetrical PRESS sequence. However, our results suggest that the remaining signal losses for the t_1 of 10 ms used experimentally are small.

Finally, a very interesting experimental finding is the phase- and intensity distorted lactate quartet of the A-nucleus with negative outer lines if the symmetrical PRESS sequence is used at $TE = 2/J$. This represents the experimental verification of the theoretically predicted existence of antiphase magnetization for the A-nucleus despite the fact that $TE = 2/J$ is used.

CONCLUSION

Localized ^{1}H NMR spectroscopy of lactate using the PRESS sequence and an echo time of $2/J$ is challenging. In theory, no signal loss occurs for the lactate doublet if the asymmetrical PRESS sequence is used and our experimental results suggest that, within our hardware restrictions, it is possible to build up such a sequence with a remaining almost negligible signal loss. The symmetrical PRESS sequence leads to the creation of NDOS as well as to PT. In theory, both effects together lead to a signal loss of up to 78% for the lactate doublet for the Hamming-filtered sinc pulses also used experimentally (75% without taking the VOD effect into account). This amount of signal loss is well confirmed by the presented experiments. A more rectangular pulse angle function, as for example obtained using RE-BURP pulses reduces the lactate doublet signal loss and makes it almost independent of single quantum polarization transfer effects. However, the influence of the VOD effect increases with improved pulses at a given slice thickness and a given slice selection gradient.

ACKNOWLEDGMENTS

Financial support by the Hans und Gertie Fischer-Stiftung and the Alfried Krupp von Bohlen und Halbach-Stiftung is gratefully acknowledged. We thank Siemens Medizintechnik, Erlangen, and the Max Grundig Clinic for continuous support.

REFERENCES

1. P. A. Bottomley, Selective volume method for performing localized NMR spectroscopy, U.S. Patent 4 480 228 (1984).
2. R. E. Gordon and R. J. Ordidge, Volume selection for high resolution NMR studies, *in* "Proceedings of the Society of Magnetic Resonance in Medicine (SMRM)," Third Annual Scientific Meeting, New York (1984), p. 272.
3. W.-I. Jung, O. Lutz, and H. Bongers, Localized proton double spin–echo spectroscopy, *in* "Proceedings of the European Society of Magnetic Resonance in Medicine and Biology (ESMRMB)," Seventh Annual Scientific Meeting, Strasbourg (1990), p. 185.
4. G. McKinnon and P. Bösiger, Lactate signal loss with echo based volume selective spectroscopy, *Magn. Reson. Med. Biol.* **4,** 101–111 (1990).
5. T. Ernst and J. Hennig, Coupling effects in volume selective ^{1}H spectroscopy of major brain metabolites, *Magn. Reson. Med.* **21,** 82–96 (1991).
6. W.-I. Jung and O. Lutz, Localized double-spin–echo proton spectroscopy of weakly coupled homonuclear spin systems, *J. Magn. Reson.* **96,** 237–251 (1992).
7. M. Bunse, W.-I. Jung, and O. Lutz, Localized double spin echo spectroscopy of weakly homonuclear coupled spin systems: Influence of chemical shift artifacts, *Appl. Magn. Reson.* **3,** 185–197 (1992).
8. D. M. Yablonskiy, J. J. Neil, M. E. Raichle, and J. H. Ackerman, Homonuclear J coupling effects in volume localized NMR spectrsocopy: Pitfalls and solutions. *Magn. Reson. Med.* **39,** 169–178 (1998).
9. M. Bunse, W.-I. Jung, O. Lutz, K. Küper, and G. J. Dietze, Polarization transfer effects in localized double-spin–echo spectroscopy of weakly coupled homonuclear spin systems, *J. Magn. Reson. A* **114,** 230–237 (1995).
10. H. Geen and R. Freeman, Band-selective radiofrequency pulses, *J. Magn. Reson.* **93,** 93–141 (1991).
11. O. W. Sørensen, G. W. Eich, M. H. Levitt, G. Bodenhausen, and R. R. Ernst, Product operator formalism for the description of NMR pulse experiments, *Progr. NMR Spectrosc.* **16,** 163–192 (1983).
12. I. Marshall and J. M. Wild, Calculations and experimental studies of the lineshape of the lactate doublet in PRESS-localized ^{1}H MRS, *Magn. Reson. Med.* **38,** 415–419 (1997).
13. R. B. Thompson and P. S. Allen, Sources of variabilty in the response of coupled spins to the PRESS sequence and their potential impact on metabolite quantification, *Magn. Reson. Med.* **41,** 1162–1169 (1999).